Swarthmore College
Works

Physics & Astronomy Faculty Works | Physics & Astronomy

11-1-2003

Test Particle Acceleration In Three-Dimensional Magnetohydrodynamic Turbulence

P. Dmitruk

W. H. Matthaeus

N. Seenu

Michael R. Brown
Swarthmore College, doc@swarthmore.edu

Follow this and additional works at: http://works.swarthmore.edu/fac-physics

Part of the Physics Commons

Recommended Citation

P. Dmitruk, W. H. Matthaeus, N. Seenu, and Michael R. Brown. (2003). "Test Particle Acceleration In Three-Dimensional Magnetohydrodynamic Turbulence". *Astrophysical Journal*. Volume 597, Issue 1. L81-L84.
http://works.swarthmore.edu/fac-physics/112

This Article is brought to you for free and open access by the Physics & Astronomy at Works. It has been accepted for inclusion in Physics & Astronomy Faculty Works by an authorized administrator of Works. For more information, please contact myworks@swarthmore.edu.

The Astrophysical Journal, 597:L81–L84, 2003 November 1
© 2003. The American Astronomical Society. All rights reserved. Printed in U.S.A.

TEST PARTICLE ACCELERATION IN THREE-DIMENSIONAL MAGNETOHYDRODYNAMIC TURBULENCE

P. Dmitruk,[1] W. H. Matthaeus,[1] N. Seenu,[1] and M. R. Brown[2]

Received 2003 June 3; accepted 2003 September 15; published 2003 October 8

ABSTRACT

We perform numerical experiments of test particle acceleration on turbulent magnetic and electric fields obtained from pseudospectral direct numerical solutions of the compressible three-dimensional MHD equations. We find consistent acceleration of the particles to many times the plasma characteristic (Alfvén) speed and extended power laws in the density distribution of energies. Scaling laws of maximum and mean energy of particles with the nominal gyrofrequency and the MHD electric field are observed and a simple estimate is presented.

Subject headings: acceleration of particles — MHD — turbulence

Understanding the mechanisms that accelerate charged particles in dynamical plasmas is an intense subject of study, with applications in astrophysical, space, and laboratory situations. Charged particles are energized in solar flares, in planetary magnetospheres, at interplanetary shocks, and in the interstellar medium. A potential contributor to this particle acceleration is magnetic field reconnection and turbulence, in which strong electric fields arise near X-type magnetic neutral points. This has been recently confirmed in the laboratory in a three-dimensional reconnection experiment (Brown et al. 2002) as well as corresponding numerical simulations (Qin et al. 2001). Coupling with simulations is useful because they can extrapolate laboratory results to larger spatial scales. Many theoretical studies have been devoted to studying the behavior of charged particles in a reconnecting field configuration (Speiser 1965; Sonnerup 1971; Vasyliunas et al. 1980; Litvinenko 1996; Somov & Kosugi 1997). Because of the complexity of particle motion in such circumstances, a useful approach has been to resort to numerical experiments based on test particle simulations, in which no interaction among the particles and no back-reaction to the imposed electromagnetic fields is considered. Investigations differ in the type of reconnection fields where the particles move. Analytical and numerical solutions have been considered in two-dimensional and three-dimensional field configurations (Sato, Matsumoto, & Nagai 1982; Scholer & Jamitsky 1989; Birn & Hesse 1994; Veltri et al. 1998; Mori, Sakai, & Zhao 1998; Schopper, Birk, & Lesch 1999; Heerikuisen, Litvinenko, & Craig 2002). Here we show and analyze new results of test particle acceleration in direct simulations of homogeneous three-dimensional MHD turbulence.

Turbulent perturbations have a distinct impact on particle acceleration by reconnection. Test particle simulations in a dynamic two-dimensional MHD current sheet, initialized with a seed population of fluctuations, indicate that turbulence can temporarily trap particles in strong electric field regions and accelerate them to large multiples of the plasma characteristic speed (Matthaeus, Ambrosiano, & Goldstein 1984; Ambrosiano et al. 1988). Broad particle energy distributions are obtained, extending to high energies. Energetic particle distributions also have been confirmed by modeled turbulent effects in Monte Carlo simulations (Kobak & Ostrowski 2000).

In fully developed turbulence, the nonlinear cascade transfers energy from large to small scales, and reconnection events are a consistently observed mode of energy dissipation (Matthaeus & Lamkin 1986). It is then of interest to address the issue of particle acceleration in homogeneous MHD turbulence, where instead of a single reconnecting site, as considered in the above-mentioned studies, many current sheet-type sites (X-points) and merging magnetic islands (O-points) may be present. The situation also relates to the process of second-order stochastic acceleration. When purely stochastic acceleration is considered for cosmic rays in galactic magnetic fields (Fermi 1949), high-energy relativistic particles are required to overcome losses due to, for instance, ionization. However, stochastic acceleration works well for both low- and high-energy particles in solar flares (Ryan & Lee 1991; Miller et al. 1997). In the situation that we are addressing, besides the second-order process, we consider an additional mechanism associated with localized intense electric field regions. Particles may be trapped in those regions by the action of turbulence, thus leading to effective acceleration even for low initial energies. This acceleration process can therefore be described (Ambrosiano et al. 1988) as consisting of both stochastic and coherent elements that interact cooperatively. Observations and simulations confirm the importance of coherent effects on particle acceleration at, for instance, the magnetosphere (Birn & Hesse 1994), solar flares (Aschwanden 2002), solar wind (le Roux, Zank, & Matthaeus 2002), and laboratory experiments (Brown et al. 2002). The consideration of both stochastic and coherent effects is also reminiscent of diffusive shock acceleration (Blandford & Eichler 1987), which is as well an effective mechanism for energizing particles.

A study of particle acceleration in homogeneous MHD turbulence was considered in Gray & Matthaeus (1992), in which numerical solutions of two-dimensional MHD were employed for the fields. Preliminary results indicated the similarity of the particle acceleration process to the earlier results for turbulent reconnection (Matthaeus et al. 1984; Ambrosiano et al. 1988). The maximum and mean energy of the particles was found to scale with the product of the nominal gyrofrequency and the Alfvén time. Power laws on the energy distribution of particles were obtained. Acceleration of particles by random localized electric fields (Anastasiadis, Vlahos, & Georgoulis 1997) is also a related study, in which a statistical cellular automata model is used instead of a direct MHD solution.

In the current study we consider the acceleration of test particles in turbulent fields obtained from a direct numerical solution of the fully three-dimensional compressible MHD equations. A large range of gyrofrequency values is employed to obtain scaling laws, which are explained by a simple estimate

[1] Bartol Research Institute, University of Delaware, 217 Sharp Lab, Newark, DE 19716; pablo@bartol.udel.edu.

[2] Department of Physics and Astronomy, Swarthmore College, 500 College Avenue, Swarthmore, PA 19081.

for the maximum and mean energies of the particles after a typical turbulence time.

The macroscopic description of a plasma given by compressible three-dimensional MHD involves a fluctuating flow velocity $\boldsymbol{v}(x, y, z, t)$, magnetic field $\boldsymbol{B}(x, y, z, t)$, and density $\rho(x, y, z, t)$. We considered periodic boundary conditions in a cube of side $2\pi L$ and take the initial magnetic fluctuation rms value B, the length scale L, and the initial mean density ρ_0 as the units of magnetic field, length, and density, respectively.[3] The Alfvén speed $v_A = B/(4\pi\rho_0)^{1/2}$ defines the unit of velocity, and the Alfvén time $t_A = L/v_A$ the unit of time. No background uniform magnetic field is assumed. The MHD equations are

$$\rho\left(\frac{\partial \boldsymbol{v}}{\partial t} + \boldsymbol{v}\cdot\nabla\boldsymbol{v}\right) = -\nabla p + \boldsymbol{J}\times\boldsymbol{B} + \frac{1}{\mathrm{R}}\left(\nabla^2\boldsymbol{v} + \frac{1}{3}\nabla\nabla\cdot\boldsymbol{v}\right), \quad (1)$$

$$\frac{\partial \boldsymbol{B}}{\partial t} = \boldsymbol{\nabla}\times(\boldsymbol{v}\times\boldsymbol{B}) + \frac{1}{\mathrm{R}_m}\nabla^2\boldsymbol{B}, \quad (2)$$

where $\mathrm{R} = v_A L/\nu$ and $\mathrm{R}_m = v_A L/\mu$ are the kinetic and magnetic Reynolds numbers, with ν the viscosity and μ the magnetic diffusivity; $\boldsymbol{J} = \boldsymbol{\nabla}\times\boldsymbol{B}$ is the current density. Continuity equation for ρ and an equation of state complete the system. We assume a nearly incompressible regime with Mach number 0.25 and treat the pressure as polytropic, $p \sim \rho^{5/3}$.

We consider a decaying simulation from an initial state with kinetic and magnetic energy per unit mass $\langle v^2\rangle = \langle B^2\rangle = 1$ (in units of v_A^2). The fluctuations initially populate an annulus in Fourier k-space such that $1 \leq k \leq 4$, with constant amplitude and random phases. We take $\mathrm{R} = \mathrm{R}_m = 1000$. We employ a pseudospectral code (Ghosh, Hossain, & Matthaeus 1993), which has been parallelized to run in a computer cluster using a scalable parallel fast Fourier transform (Dmitruk et al. 2001). The resolution is 256^3 Fourier modes, which guarantees that the dissipation scales are fully resolved for the moderate Reynolds numbers considered. After $2t_A$ times, a fully turbulent state with a broad range of scales has been developed. The magnetic field for the particle motion is directly obtained from the numerical solution, while the electric field $\boldsymbol{E}$ is obtained through Ohm's law,

$$\boldsymbol{E} = -\boldsymbol{v}\times\boldsymbol{B} + \frac{1}{\mathrm{R}_m}\boldsymbol{J}. \quad (3)$$

The electric field is expressed in units of $v_A\bar{B}/c$ (c is the speed of light) and is the result of the induced part due to the plasma motion plus a formally small resistive term that is important in current sheet regions. Visualizations (front-side planes of the simulation box) of the magnetic field $|\boldsymbol{B}|$ and the electric field $|\boldsymbol{E}|$ are shown in Figure 1. The electric field is a much more intermittent quantity with high values observed in a less space-filling distribution. Both fields show a broad range of length scales present and a high degree of complexity. The energy spectrum of the MHD fields (not shown) is consistent with a

[3] The value of L is of the same order as the energy containing scale or the magnetic field correlation length, which is approximately constant throughout the short time evolution of the system. This gives physical meaning to the chosen unit length.

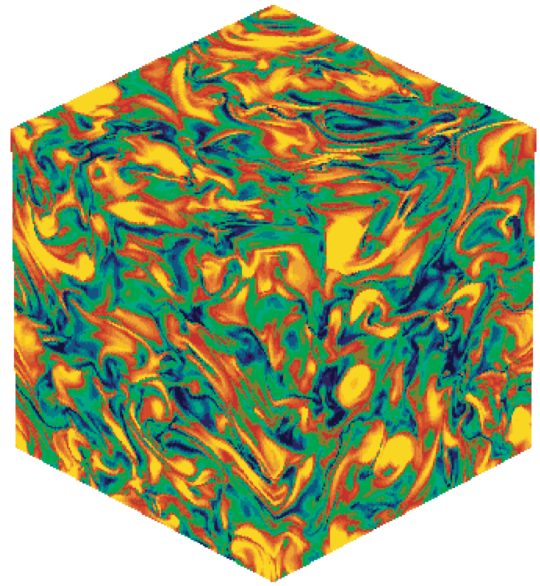

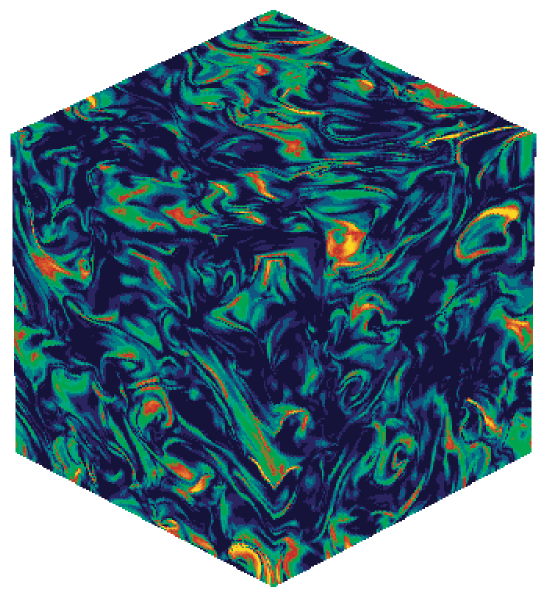

FIG. 1.—Visualization of the turbulent magnetic field $|B|$ (*top*) and electric field $|E|$ (*bottom*) in the simulation box. High values are in yellow (*light*) and low values in blue (*dark*).

Kolmogorov 5/3 power law. This turbulent state of the system that is achieved after two eddy turnover times is used as an external field for pushing the test particles.

The nonrelativistic equations of motion for the charged particles in the fields are

$$\frac{d\boldsymbol{u}}{dt} = \alpha(\boldsymbol{u}\times\boldsymbol{B} + \boldsymbol{E}), \quad \frac{d\boldsymbol{x}}{dt} = \boldsymbol{u}, \quad (4)$$

with $\alpha = \Omega_i t_A$, where $\Omega_i = q_i\bar{B}/m_i c$ is the nominal gyrofrequency (with q_i and m_i the particle charge and mass). We use the same units as in the MHD equations with the particle

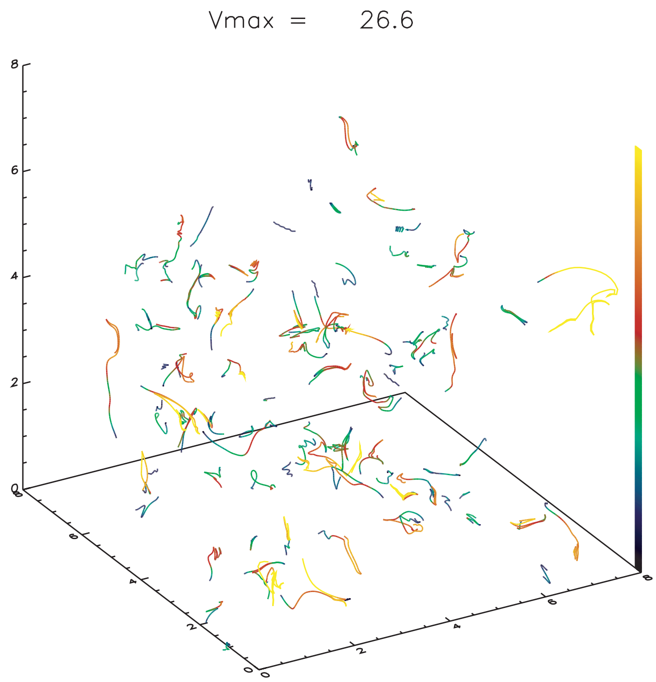

FIG. 2.—Trajectories of 100 test particles (out of 50,000) from the simulation, with colors indicating the particles' speed.

velocity $\boldsymbol{u}$ in Alfvén speed v_A units. The dimensionless quantity, $\alpha = \Omega_i t_A$, relates the turbulent field scales with the particle motion scales. In general, $\alpha \gg 1$; that is, the turbulent timescales are much slower than the typical gyroperiods of particles. We consider 50,000 particles and values of $\alpha = 10^2$, 10^3, 10^4, and 10^5. The particles are moved using a Runge-Kutta fourth-order time integration method, with an adaptive time step calculation. The code is parallelized by sending particles to each processor to solve the trajectory during an interval $\Delta t = 0.5 t_A$ starting from $t = 2t_A$ in the MHD solution. The values of the magnetic and electric field at each particle position are obtained by linear interpolation in space from the grid of the MHD simulation. We start from an initial monoenergetic particle population, with speed $|\boldsymbol{u}| = v_A$ and random (isotropically distributed) direction, and their positions are randomly distributed in the simulation box of size $2\pi L$. Since we consider homogeneous MHD turbulence, the electric and magnetic fields are periodically replicated in space, so the values can be readily obtained if a particle leaves the initial region. However, the distance traveled by the particles during the time of the simulation (of the order of the turbulent correlation timescale) is less or about L (see Fig. 2 for a sample of particle trajectories), which means that they are not repeatedly subject to the same field values. Trajectories of the particles (for a case with $\alpha = 10^4$) are shown in Figure 2, where 100 particles have been selected for the plot. The colors in the trajectories correspond to the particle speed. It can be seen that some particles are not highly accelerated at all, while others reach speeds much higher than the plasma characteristic speed v_A. It is also seen, on comparison with the turbulent fields (Fig. 1), that each particle encounters or moves only through a single region where the fields vary appreciably; that is, particles do not sample many regions of turbulent field activity in the box during the simulation. That situation will not hold on longer timescales, where

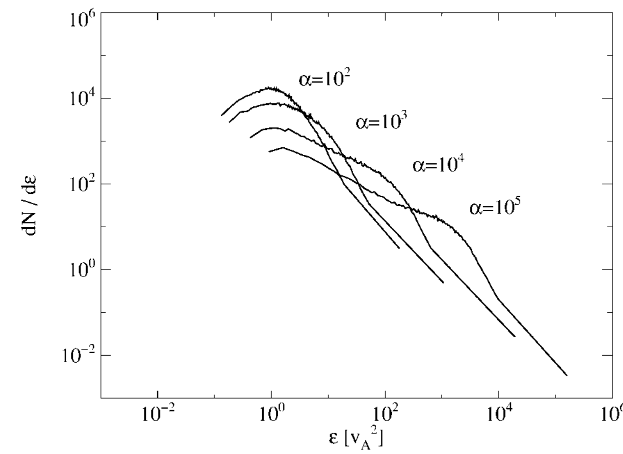

FIG. 3.—Particle energy distribution for different values of $\alpha = \Omega_i t_A$ after an interval $\Delta t = 0.5 t_A$.

a description based on diffusion might be appropriate. It is not the aim of this Letter to investigate such issues, but we mention in passing theoretical antecedents that consider a Fokker-Planck description (Hall & Sturrock 1967; Achatz, Steinacker, & Schlickeiser 1991; Schlickeiser & Miller 1998).

We compute the particle energy (per unit mass) distribution $dN/d\epsilon$, where $\epsilon = u^2$. This is shown in Figure 3 for different values of $\alpha = \Omega_i t_A$, after an interval $\Delta t = 0.5 t_A$. For the smallest $\alpha = 10^2$ case, the distribution is a power law $\approx \epsilon^{-2}$ at high energies, but as α is increased a flatter power law $\approx \epsilon^{-0.6}$ emerges. A high-energy tail remains $\approx \epsilon^{-2}$ but shifted to increasingly higher energies. Maximum and mean energy achieved by the particles for different values of α is shown in Figure 4. An approximate linear behavior is seen.[4]

[4] It should be cautioned that the calculation was not made for relativistic particles, so values cannot be extrapolated here to high values of V_A compared to c.

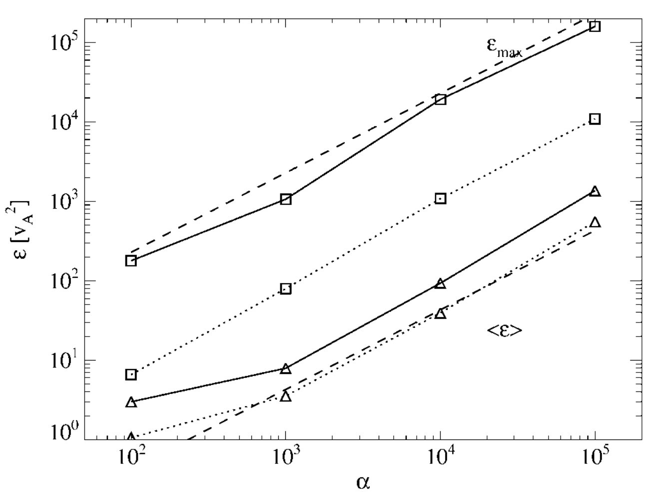

FIG. 4.—Maximum (*squares on the solid line*) and mean energy (*triangles on the solid line*) of the particles for different values of $\alpha = \Omega_i t_A$ after $\Delta t = 0.5 t_A$. Squares and triangles over the dotted lines show the maximum and mean energy obtained from particle simulations considering only the ohmic part of the electric field. The dashed lines correspond to the energy estimates as explained in the text.

In order to get insight of whether the results are controlled by the ohmic part of the electric field (the term $\boldsymbol{J}/\mathrm{R}_m$ in eq. [3], which contains the parallel component to the local magnetic field) or by the induced part $-\boldsymbol{v} \times \boldsymbol{B}$, which is strictly perpendicular to $\boldsymbol{B}$, we performed an additional set of test particle simulations, in which the induced electric field is (artificially) put to 0. The results for the maximum and mean energy of those runs are shown by the squares and triangles over the dotted lines in Figure 4. It is clear that the ohmic part alone cannot give the proper answer for the maximum and mean energy and the contribution from the induced electric field is relevant, especially for the maximum energies, which are off by more than an order of magnitude in the "ohmic-only" case.

We propose two physically motivated mechanisms to estimate, in order of magnitude, the mean and maximum energy scalings. For the mean energy, we assume that the particle encounters a region where the electric field is coherent over some correlation length. In this case, the perpendicular field acts only to "confine" the motion in those regions, but the energy increase comes from the parallel field. We integrate the change of speed equation $du^2/dt = 2\alpha E_\parallel$ to obtain (initial speed is assumed small compared to the speed change) $\epsilon = u^2 \sim \alpha^2 E_\parallel^2 t_*^2$, where the coherence time t_* is given by the motion along a parallel correlation length, $\lambda_\parallel \sim \frac{1}{2}\alpha E_\parallel t_*^2$. The energy is then $\epsilon \sim 2\alpha E_\parallel \lambda_\parallel$, which is linear in α. This is analogous to the mechanism in two-dimensional turbulent reconnection given by Matthaeus et al. (1984) and Ambrosiano et al. (1988). For the maximum energy a complementary mechanism is proposed here. The role of the perpendicular field is more important in this case (see Fig. 4). In particular, if a particle enters a reconnection site, the action of the plasma inflow $\boldsymbol{v}$ at both sides of the reconnection zone and the local main field $\boldsymbol{B}$ produces a perpendicular electric field $\boldsymbol{E} = -\boldsymbol{v} \times \boldsymbol{B}$ that reverses sign across the reconnection zone (where a net current $\boldsymbol{J}$ parallel to $\boldsymbol{B}$ is sustained, the current being given by $\boldsymbol{\nabla} \times \boldsymbol{b}$ of the fluctuations $\boldsymbol{b}$, the reconnecting part of the field). A particle orbiting around $\boldsymbol{B}$ will receive kicks by this reversing electric field, thus increasing the particle energy in a resonant way. Integrating the change of speed equation $du^2/dt = 2\alpha u E$ produced by the successive kicks over an interval t_*, which is given by the motion along a parallel correlation length $\lambda_\parallel$, we obtain $\epsilon_{\max} \sim \alpha 2 \lambda_\parallel E^2/E_\parallel$ (we assume that the parallel extent of the reconnection site is $\lambda_\parallel$). A crucial distinction with respect to the mean energy is that the field E here refers to the main perpendicular part in the reconnection zone. If we use $E_\parallel \sim aE$ and $\lambda_\parallel \sim bL$, where a, b are small numerical factors ($a, b \approx 0.1$ in our case), we obtain $\epsilon_{\max} \sim 2\alpha EL$, which is linear in α. The mechanism described is idealized and may be more complex in a turbulent state; however, acceleration by a more general nonuniform perpendicular electric field may proceed in essentially the same way. In that case, particles orbiting around $\boldsymbol{B}$ receive kicks (although not exactly resonant) by the nonuniform perpendicular electric field that gives a net acceleration. Nonuniform magnetic fields may also play a role through mirroring effects on the parallel motion. In Figure 4 (*dashed lines*) we show the estimated scalings for the mean and maximum energies. The mean energy estimate ignores the effect of the high-energy particles given by the induced electric field, so the values lie actually closer to the ohmic-only computation. The maximum energy can be rewritten as $\epsilon_{\max}(\mathrm{eV}) \sim vBL$, with v a typical plasma speed in m/s, B in T, and L in m. It is interesting that this is consistent with the scaling observed in the Swarthmore Spheromak laboratory reconnection experiment (Brown et al. 2002) and a wide range of space and astrophysical systems (Makishima 1999).

In summary, our results show that three-dimensional MHD turbulence can efficiently accelerate particles in relatively short times, with velocities reaching many times the plasma characteristic (Alfvén) speed and extended power laws in the distribution of energies. Linear scaling laws of mean and maximum energy with the nominal gyrofrequency and the electric field are obtained, as well as an estimate based on encounters with regions of coherent electric fields over typical correlation lengths and nonuniform perpendicular electric fields in reconnection sites. Although additional effects would be needed to apply this basic study to particular applications, it provides a building block for understanding energetic particles in astrophysical, space, and laboratory situations.

Research supported by NASA NAG5-7164, NSF ATM-0105254, ATM-9977692, and DOE FG02-98ER54490. Runs performed on Beowulf clusters at Bartol Research Institute, University of Delaware.

REFERENCES

Achatz, U., Steinacker, J., & Schlickeiser, R. 1991, A&A, 250, 266
Ambrosiano, J., Matthaeus, W. H., Goldstein, M. L., & Plante, D. 1988, J. Geophys. Res., 93, 14,383
Anastasiadis, A., Vlahos, L., & Georgoulis, M. K. 1997, ApJ, 489, 367
Aschwanden, M. J. 2002, Space Sci. Rev., 101, 1
Birn, J., & Hesse, M. 1994, J. Geophys. Res., 99, 109
Blandford, R., & Eichler, D. 1987, Phys. Rep., 154, 1
Brown, M. R., Cothran, C. D., Landreman, M., Schlossberg, D., & Matthaeus, W. H. 2002, ApJ, 577, L63
Dmitruk, P., Wang, L.-P., Matthaeus, W. H., Zhang, R., & Seckel, D. 2001, Parallel Computing, 27, 1921
Fermi, E. 1949, Phys. Rev., 75, 1169
Ghosh, S., Hossain, M., & Matthaeus, W. H. 1993, Comput. Phys. Commun., 74, 18
Gray, P. C., & Matthaeus, W. H. 1992, in AIP Conf. Proc. 264, Particle Acceleration in Cosmic Plasmas, ed. G. P. Zank & T. K. Gaisser (Melville: AIP), 261
Hall, D. E., & Sturrock, P. A. 1967, Phys. Fluids, 10, 2620
Heerikuisen, J., Litvinenko, Y. E., & Craig, I. J. D. 2002, ApJ, 566, 512
Kobak, T., & Ostrowski, M. 2000, MNRAS, 317, 973
le Roux, J. A., Zank, G. P., & Matthaeus, W. H. 2002, J. Geophys. Res., 107, 1138
Litvinenko, Y. E. 1996, ApJ, 462, 997
Makishima, K. 1999, Astron. Nachr., 320, 163
Matthaeus, W. H., Ambrosiano, J. J., & Goldstein, M. L. 1984, Phys. Rev. Lett., 53, 1449
Matthaeus, W. H., & Lamkin, S. L. 1986, Phys. Fluids, 29, 2513
Miller, J. A., et al. 1997, J. Geophys. Res., 102, 14,631
Mori, K.-I., Sakai, J.-I., & Zhao, J. 1998, ApJ, 494, 430
Qin, G., Lukin, V. S., Cothran, C. D., Brown, M. R., & Matthaeus, W. H. 2001, Phys. Plasmas, 8, 4816
Ryan, J. M., & Lee, M. A. 1991, ApJ, 368, 316
Sato, T., Matsumoto, H., & Nagai, K. 1982, J. Geophys. Res., 87, 6089
Schlickeiser, R., & Miller, J. A. 1998, ApJ, 492, 352
Scholer, M., & Jamitsky, F. 1989, J. Geophys. Res., 94, 2459
Schopper, R., Birk, G. T., & Lesch, H. 1999, Phys. Plasmas, 6, 4318
Somov, B. V., & Kosugi, T. 1997, ApJ, 485, 859
Sonnerup, B. U. O. 1971, J. Geophys. Res., 76, 8211
Speiser, T. W. 1965, J. Geophys. Res., 70, 4219
Vasyliunas, V. M. 1980, J. Geophys. Res., 85, 4616
Veltri, P., Zimbardo, G., Taktakishvili, A. L., & Zelenyi, L. M. 1998, J. Geophys. Res., 103, 14,897